Supplementary information for

Diurnal variation of aerosol indirect effect for warm marine boundary layer clouds in the eastern north Atlantic.

Shaoyue Qiu, Xue Zheng, David Painemal, Christopher R. Terai, and Xiaoli Zhou

[1]Atmospheric, Earth and Energy Division, Lawrence Livermore National Laboratory, Livermore, California, USA
[2] Science Directorate, NASA Langley Research Center, Hampton, VA, USA
[3] Analytical Mechanics Associates, Hampton, VA, USA
[4]Chemical Sciences Laboratory, NOAA, Boulder, CO, USA,
[5]Cooperative Institute for Research in Environmental Sciences (CIRES), University of Colorado, Boulder, CO, USA

This file includes:

Supplementary text

Figs. S1 to S6

Supplementary Text

Evaluation of Meteosat-11 cloud mask with ARM ground-based observations.

As the cloud fraction (CF) in Meteosat is defined as areal fraction of each time step, while CF from the ground-based radar-lidar observations is defined as the percentage of time when clouds are detected. To enable comparison, we calculate the CF from Meteosat over a $0.5° \times 0.5°$ grid box centered at the ground site. For ground-based observations, CF is computed over a one-hour period centered at each Meteosat cycle (e.g., Dong et al., 2002, 2016; Xi et al., 2010). Since Meteosat is unable to observe low clouds below an upper cloud layer, boundary layer clouds in ARM ground-based observations are defined as clouds with the radar detected uppermost cloud tops below 3km to be consistent with satellite definition. In Figure S1, we present the average diurnal variation of boundary layer clouds derived from Meteosat and ARM ground-based observation during the four-month study period from 2018 to 2021 in July.

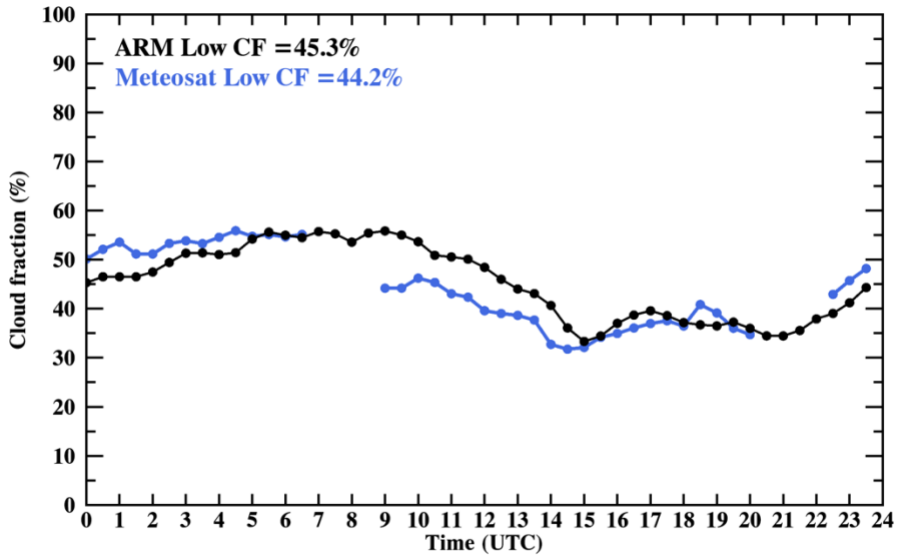

Figure S1: Diurnal variation of boundary layer cloud fraction derived from the ground-based radar-lidar-ceilometer measurements at the Atmospheric Radiation Measurement Eastern North Atlantic (ARM ENA) site (black line) and from Meoteosat-11 (blue line).

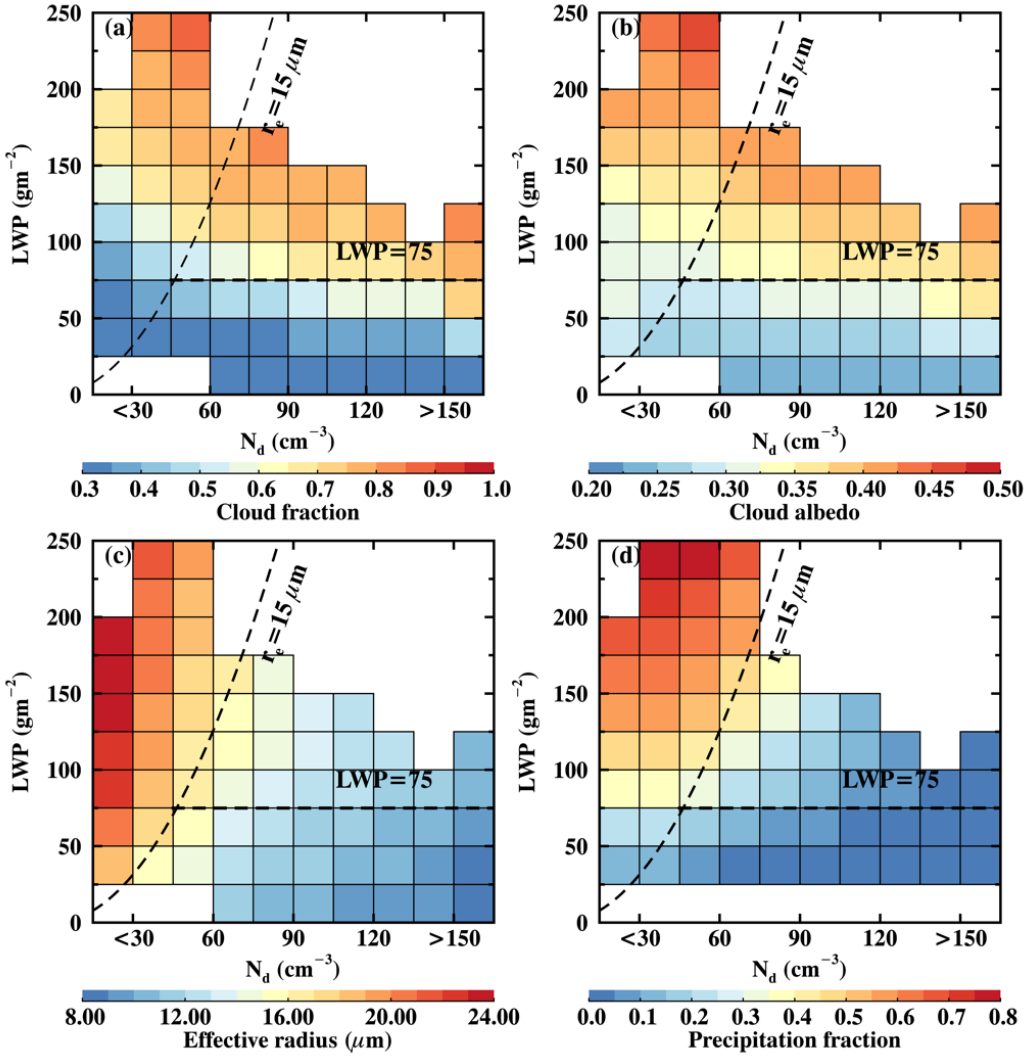

Figure S2. Daytime mean cloud properties for different N_d and LWP bins. (a) cloud fraction (b) cloud albedo, (c) effective radius, and (d) pixel-level precipitation fraction. The dashed lines indicate r_e =15 μm and LWP= 75 gm^{-2}, as thresholds for precipitation (precipitating clouds located to the left of the line) and thick clouds (with LWP > 75 gm^{-2}).

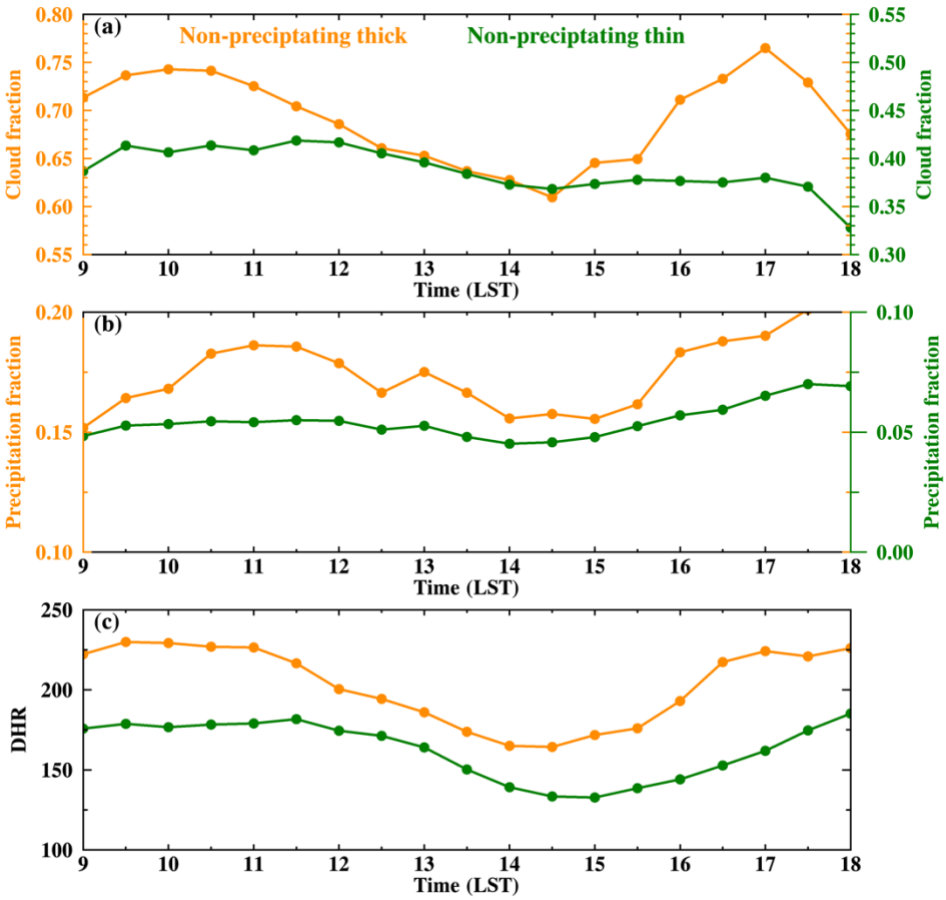

Figure S3. Diurnal variation of (a) cloud fraction, (b) pixel-level precipitation fraction, and (c) diameter-to-height ratio (DHR) for non-precipitating clouds. Different colors represent different cloud states as indicated in (a). Please note that the non-precipitating thin cloud in (a) and (b) use the y-axis on the right side.

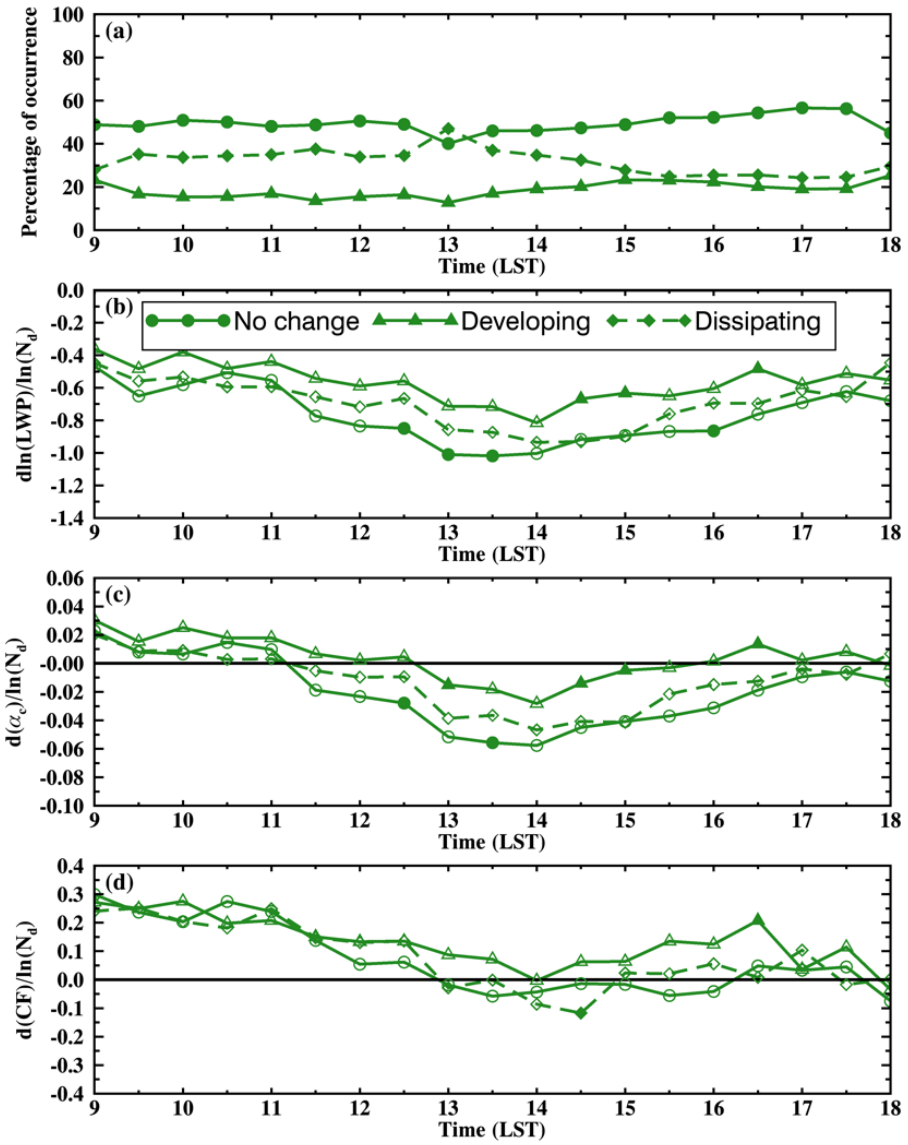

Figure S4. Daytime variation of non-precipitating thin clouds that have small changes in the 1° × 1° mean cloud fraction (CF) (No change, solid line with circle symbols), with an increase in the mean CF (developing, solid line with triangle symbols), and with a decrease in the mean CF (dissipating, dash line with diamond symbols) within a 30-minute window. (a) Percentage of occurrence for the three groups above, (b) cloud LWP susceptibility ($dln(LWP)/dln(N_d)$), (c) cloud albedo susceptibility ($d\alpha_c/dln(N_d)$), and (d) cloud fraction susceptibility ($dCF/dln(N_d)$) for non-precipitating thin clouds. Symbols representing different cloud stages are noted in (b). In (b)-(d), filled markers indicate data points that are significantly different from the other two groups ($p<0.05$). Open markers indicate statistical insignificance.

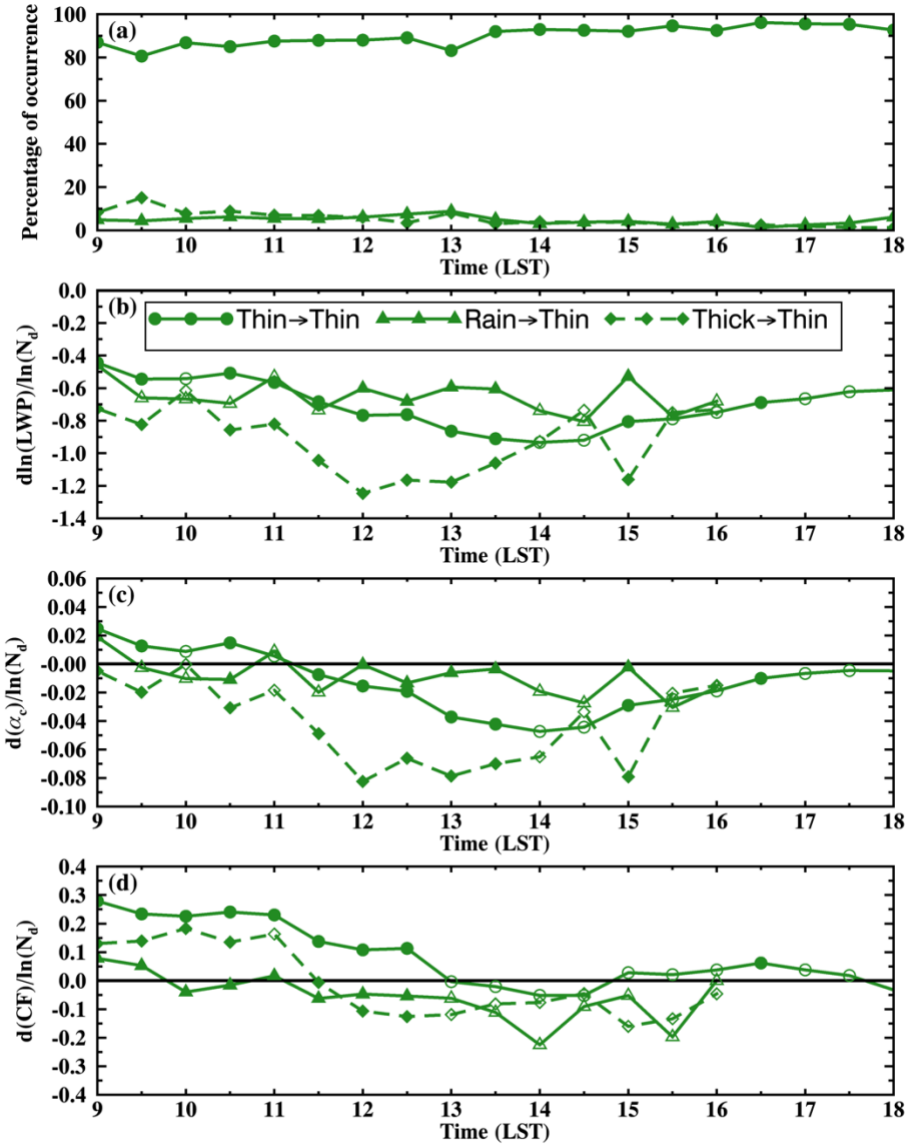

Figure S5. Daytime variation of non-precipitating thin clouds transition from non-precipitating thin clouds (thin → thin, solid line with circle symbols), precipitating clouds (rain → thin, solid line with triangle symbols), and non-precipitating thick clouds (thick → thin, dash line with diamond symbols) in previous half an hour. (a) Percentage of occurrence for the three groups above, (b) cloud LWP susceptibility ($dln(LWP)/dln(N_d)$), (c) cloud albedo susceptibility ($d\alpha_c/dln(N_d)$), and (d) cloud fraction susceptibility ($dCF/dln(N_d)$) for non-precipitating thin clouds. Symbols for different state transitions are noted in (b). In (b)-(d), filled markers indicate data points that are significantly different from the other two groups ($p<0.05$), while open markers indicate statistical insignificance.

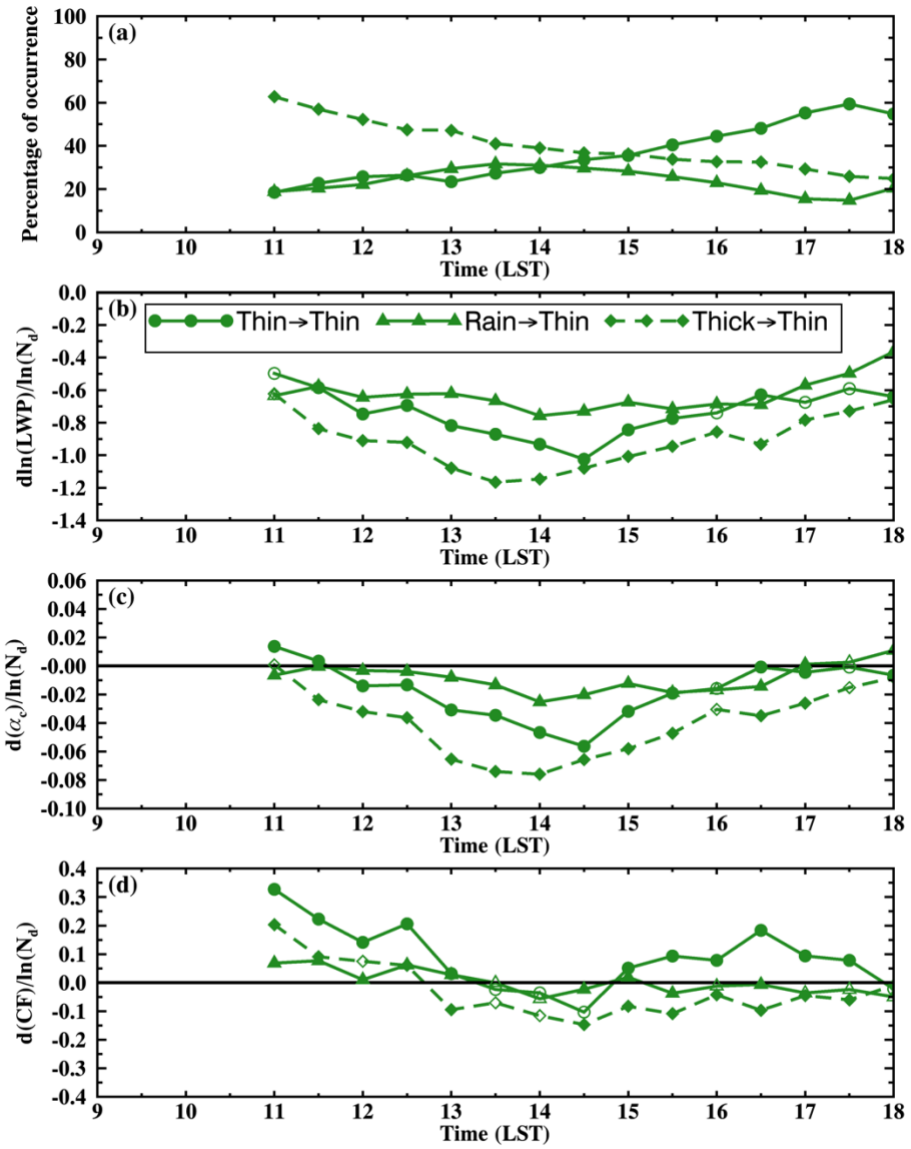

Figure S6. Daytime variation of non-precipitating thin clouds transition from non-precipitating thin clouds (thin → thin, solid line with circle symbols), precipitating clouds (rain → thin, solid line with triangle symbols), and non-precipitating thick clouds (thick → thin, dash line with diamond symbols) in previous four hours. (a) Percentage of occurrence for the three groups above, (b) cloud LWP susceptibility ($dln(LWP)/dln(N_d)$), (c) cloud albedo susceptibility ($d\alpha_c/dln(N_d)$), and (d) cloud fraction susceptibility ($dCF/dln(N_d)$) for non-precipitating thin clouds. Symbols for different state transitions are noted in (b). In (b)-(d), filled markers indicate data points that are significantly different from the other two groups ($p<0.05$), while open markers indicate statistical insignificance. The lack of definition of cloud state transition between 9-11 LST is due to filtering of cloud retrievals with the SZA threshold.